Indonesian Journal of Physics
Vol 22 No. 3, July 2011

Characteristics of a Metal-Dielectric-Metal Slab Waveguide with Embedded Metallodielectric Photonic Crystal and its Optimization at Low THz Optical Frequency

Teguh P. Negara[1,3], Mardanih[2,3], Hendradi Hardhienata[3], Husin Alatas[3,#]
[1)]Computer Science Department, Faculty of Mathematics and Natural Sciences, Pakuan University, Bogor, Indonesia
[2)] Lembaga Bimbingan & Konsultasi Belajar Nurul Fikri, Bogor, Indonesia
[3)]Theoretical Physics Division, Departement of Physics, Bogor Agricultural University,
[#)]Corresponding author: alatas@ipb.ac.id

Received 3 February 2011, Revised 15 April 2011, Accepted 18 May 2011

Abstract

In this paper we report the results of our systematic numerical study on the characteristics of a metal-dielectric-metal slab waveguide with an embedded 1D metallodielectric photonic crystal using finite difference time domain method. At low terahertz (THz) optical frequency, the results show that the sensitivity of the device depends significantly on the shape of the corresponding dielectric rod, which acts as a defect, and the distance between the two metallic rods. In this simulation, the optimum device sensitivity is obtained for a round shaped defect with a radius of 0.28 mm lattice constant of 0.35 mm and operational frequency of 2.69 THz which lies in the range of bio-molecule vibrational mode.

Keywords: *Metal-Dielectric-Metal Slab Waveguide; One-Dimensional Metallodielectric Photonic Crystal; FDTD method; THz Optical Frequency.*

1. Introduction

An intensive research area in modern photonics has offered the ability to control light in the wavelength and sub-wavelength scales[1)]. In the mean time, due to high concentration of free electrons, metals have unique optical properties since the collective vibration of electrons in metallic materials can cause interesting effects. One of them is the electronic density fluctuation at the interface between metal and dielectric materials called surface plasmons[1-3)].

The existence of surface plasmons in metallic layered structure has been widely studied, such as in the binary metallic grating with a small gap used as optical filter or biosensor[3)] or metal-dielectric-metal (MDM) as cavity or waveguide in photonic devices[1,4)]. It is known theoretically that one dimensional (1D) photonic crystal made from metal exhibits nonlinear optical response[5)]. This phenomenon has also been proven experimentally in[6)]. Meanwhile, it has been reported in[7-9)] that 1D photonic crystal with inserted defect layers can be applied as a sensor due to defect resonances. On the other hand, recent progress in terahertz (THz) optics offers the possibility to probe the underlying physical mechanism inside bio-molecules which have vibrational modes in low THz frequency range[10,11)].

Based on these facts, in this report, we discuss the characteristics of MDM slab waveguide with embedded 1D metallodielectric photonic crystal. The corresponding photonic crystal consists of 10 square metallic rods and a dielectric defect rod inserted in the middle. At low THz optical frequency, the finite difference time domain (FDTD) simulation results shows that the sensing sensitivity of the proposed structure can be optimized by choosing proper values for the defect shape and dimension, as well as the lattice constant, a, i.e. the distance between two adjacent square metallic rods.

2. Numerical Formulation and Measured Output Parameters

It is well-known that electromagnetic wave propagation inside photonic crystal systems can be described by the four Maxwell equations. Here, we solve the Maxwell equation by using the FDTD method[14)] and only limit our self to the TM polarization case where the electric field $\vec{E}(x,y)$ is oscillating in the x-y plane and the magnetic field $\vec{H}(x,y)$ is oscillating along the z - axis. It is important to note that the surface plasmons occur only in the TM polarization mode with $\vec{E}=(E_x, E_y, 0)$ and $\vec{H}=(0,0,H_z)$.

Based on the Yee algorithm[12)], and the perfectly matched layer (PML)[13)] as the chosen boundary condition, the corresponding Maxwell equations to be discretized can be written in the following form[14)]:

$$i\omega\left[1+\frac{\sigma_p(x,y)}{i\omega\varepsilon_0}\right]H_z=\frac{1}{\mu_0}\left(\frac{\partial E_x}{\partial y}-\frac{\partial E_y}{\partial x}\right) \quad (1)$$

$$i\omega\left[1+\frac{\sigma_p(x,y)}{i\omega\varepsilon_0}\right]^{-1}D_x=\frac{\partial H_z}{\partial y} \quad (2)$$

$$i\omega\left[1+\frac{\sigma_p(x,y)}{i\omega\varepsilon_0}\right]^{-1} D_y = -\frac{\partial H_z}{\partial x} \quad (3)$$

with $D_x = g\varepsilon_0 E_x$, $D_y = g\varepsilon_0 E_y$ and $g = [\varepsilon_r(x,y)+\sigma(x,y)dt/\varepsilon_0]^{-1}$, while σ_p, σ and ε_r denote the PML parameter, material conductivity and the relative permittivity of the material, respectively, while ω is the operational frequency.

To observe the change in the electric field due to variations of the device parameters, we consider the total output energy at the right-end side of the device as a function of time defined as[8,9]:

$$Q(t) = \int_0^h \varepsilon_0\varepsilon_r \left|\vec{E}(t)\right|^2 dy \quad (4)$$

with $\left|\vec{E}\right| = \sqrt{|E_x|^2 + |E_y|^2}$ and h is the thickness of the dielectric slab. We then define a parameter that describes the average energy density for a certain amount of time, as follows[8,9]:

$$W = \frac{1}{t}\int_0^t Q(t)dt \quad (5)$$

3. Device Model

The corresponding device model is presented in Figure 1. We considered a dielectric slab with metallic cladding and ten metallic rods arrayed with lattice constant a in one direction inside the slab along with one dielectric defect rod of refractive index n the middle which considered as a receptor. The system is illuminated by a continuous electromagnetic field from the left side which will be guided perfectly inside the dielectric slab by the metallic claddings.

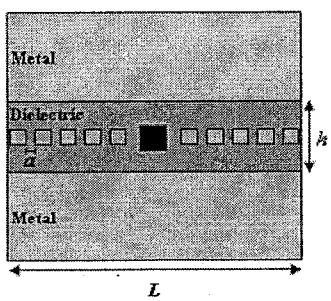

Figure 1. Sketch of the device considered. The black rod is a dielectric defect rod with refractive index n, while a denote the lattice constant (distance between two adjacent square metallic rods).

In our numerical calculation, we adopt the model of metallic material permittivity described by the following Drude's formula[15]:

$$\varepsilon_r = 1 - \frac{\omega_p^2}{\omega^2 + i\gamma\omega} \quad (6)$$

where ω_p denotes the angular plasma frequency and γ^{-1} is related to the relaxation time of the electrons[15], and we use $\omega_p = 1419$ THz and $\gamma = 134.9$ THz[16]. Here, the metallic material considered is assumed to be nonmagnetic with $\mu_r = 1$, while the dielectric slab is assumed to have relative permittivity of $\varepsilon_r = 12.11$. The length of the structure is $L = 11.9$ mm.The thickness of the dielectric layer is $h = 2.1$ mm, while the metallic claddings are semi-infinite in y- direction. The dimension of each square metallic rods is 0.7×0.7 mm^2, and the lattice constant $a = 0.35$ mm.

In the simulation, we use 400×400 meshes, where each of the mesh has a dimension of $\Delta x = \Delta y = 35$ μm. For the time step we set $\Delta t = 5.83 \times 10^{-5}$ ps and the output is measured at $t = 1.1667 \times 10$-1- ps..

4. Results and Discussions

The response characteristic of the corresponding device at the output is depicted in Figure 2. It is shown that W depends on the operational frequency. Clearly from the figure that for the range of 0.05 - 3THz the device admits high W, while for the range of 3-2000 THz low W is obtained, except around the plasma frequency ω_p = 1419 THz. We believe that this wide "band-gap" with low W exists due to both wave absorption by the metallic structure and destructive interference mechanism between the forward and backward propagating waves.

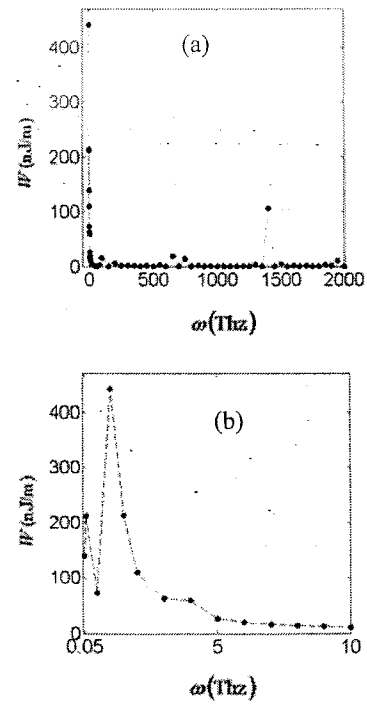

Figure 2. Relation between W and the variation of operational frequency for the range of (a) 0.05-2000 THz and (b) 0.05-10 THz. Note that we used a non-uniform increment.

It is well known that the surface plasmons occur when the real part of the metal permittivity is negative namely at $\omega < \omega_p$ [2,15], which for this case is given at the range of ω < 1412.5THz obtained from the Drude's model given by Eq. (6). In this condition, the wave experience small attenuation on the metallic surface. Therefore, in the next simulation, ω = 2.69 THz is chosen to be the operational frequency which lies in the range of the vibrational mode of bio-molecule such as protein[10,11].

Figure 3 shows the value of W at the output of the structure as a function of the defect index, n. For a square defect rod, W tends to increase if n increases. The contrary is observed for a round defect rod where W decreases for increasing n. Figure 3 also shows that the round defect rod has a steeper gradient for the same defect index interval. This result describes that this shape is more sensitive than the square one. Therefore, this round defect shape will be our focus in the next discussion.

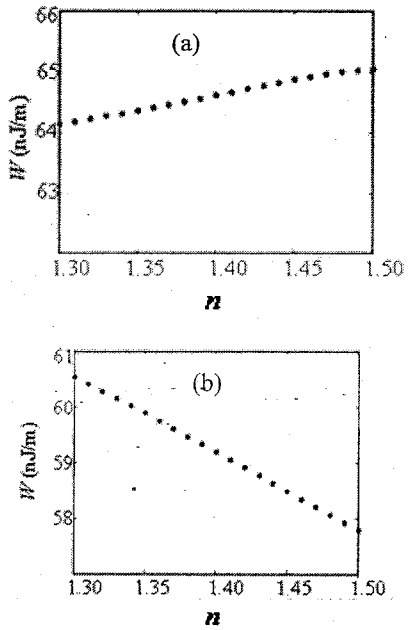

Figure 3. W as a function of defect refractive index of (a) square defect rod with a side length of 0.7mm, (b) round defect rod with a radius of 0.28 mm.

To investigate the output characteristic with respect to n, we choose the range of n = 1.30 to 1.50, which is generally related to a liquid sample of bio-substance. Figure 4 depicts the relation between the round defect radius on W at the output. This test is performed by observing the change in W as a function of n for different radius. The simulation shows that a defect radius of 0.28 mm is more effective because W has a steeper gradient. Meanwhile for a defect radius of 0.14 mm and 0.07 mm, no significant change in W is observed, thus this parameter setting is ineffective as an index sensor.

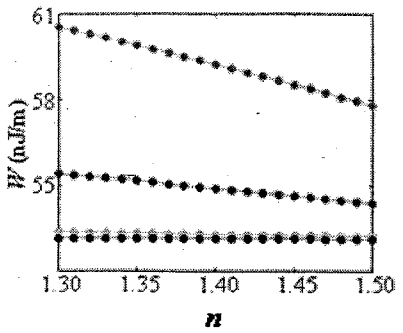

Figure 4. (Color online) Dependence of the round defect rod radius on W for a defect index of 1.30 with radius of 0.28 mm (red), 0.21 mm (blue), 0.14 mm (black) and 0.07 mm (green).

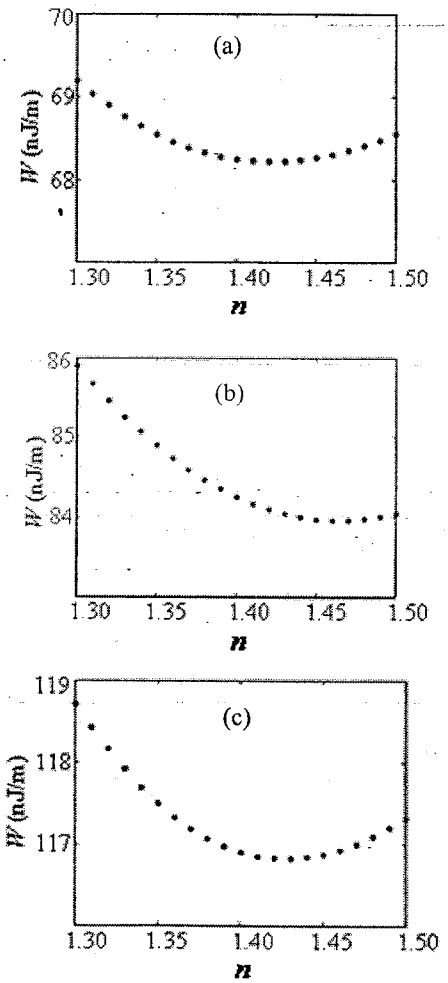

Figure 5. W as a function of the defect index with lattice constant of (a) 0.21mm (b) 0.14mm (c) 0.035mm.

For the investigation of the effect of lattice constant on the response characteristics of the device for the given range of n, we consider three more different values of the lattice constants namely: 0.21 mm, 0.14 mm and 0.035 mm. As demonstrated in

Figure 5, decreasing the distances will lead to the larger value of W, while the response is no longer linear in the given range. Although it is not clear for us at this moment, but probably this characteristic is related to a large field enhancement due to interaction between the surface plasmons of two adjacent square metallic rods when both getting closer. Depicted in Figure 6 is an example of large field enhancement phenomenon for a system of two square metallic rods embedded in a homogeneous dielectric media with ε_r = 12.11, where each of them have the same 0.7 × 0.7 mm^2 size and separated by a distance of 0.35 mm.

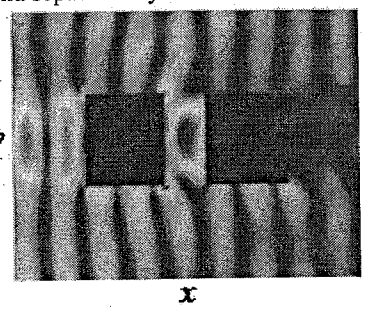

Figure 6. (Color online) Snapshot of the field intensity distribution in a system of two square metallic rods embedded in homogeneous dielectric media, showing large enhancement in the space between the two rods.

5. Summary

We have demonstrated that the proposed system of a metal-dielectric-metal slab waveguide with embedded 1D metallodielectric photonic crystal exhibits optical band-gap for a certain operational frequency range which is likely occur due to both metallic attenuation and destructive interference between the forward and backward propagating waves. We found that the sensing performance of the device in the low THz optical frequency region outside the band-gap can be optimized by choosing a round defect rod instead of the square shape. It is observed that for smaller lattice constant, the value of average energy density becomes larger, while the corresponding response is no longer linear. One may expect that the combination of the sensing mechanism discuss in this report and the absorption of bio-molecule in the liquid sample at low THz optical frequency can lead to the enhanced performance of the device.

Acknowlegdement

T. P. Negara would like to thank Faculty of Mathematics and Natural Sciences, Pakuan University, for financial support.

References

1. Y. Todorov *et al.,* Optical properties of metal-dielectric-metal microcavities in the THz frequency range, *Opt. Expr* **13**, 13886, 2010.
2. J. Smajic *et al.,* Comparison of Numerical Methods for the Analysis of Plasmonic Structures, *J. Comput. Theor. Nanosci.* **6**, 1, 2009.
3. V. M. Fitio, H. P. Laba, and V. V. Bobotski, Electromagnetic resonance absorption in metallic gratings, *Semiconductor Phys. Quant. Electron. Optoelectron.* **9**, 49, 2006.
4. Z. Han, and S. He, Multimode interference effect in plasmonic sub-wavelength waveguides and an ultra-compact power splitter, *Opt. Comm.* **278**, 199, 2007.
5. R. S. Bennink, *et al.,* Accessing the optical nonlinearity of metals with metal–dielectric photonic bandgap structures, *Opt. Lett* **24**, 1416, 1999.
6. N. N. Lepeshkin *et al.,* Enhanced nonlinear optical response of one-dimensional metal-dielectric photonic crystals, *Phys. Rev. Lett.* **93**, 123902, 2004.
7. H. Alatas *et al.,* Single-frequency refractive index sensor based on a finite one-dimensional photonic crystals with two defects, *Jpn. J. Appl. Phys.* **45**, 8B, 6754, 2006
8. Mardanih *et al.,* Characteristics of 1D photonic crystal sensor with Two defect, *AIP Conf. Proc.* **1325**, 313, 2010
9. T. P. Negara *et al.,* Transmission characteristics of 1D metallodielectric photonic crystal with a defect rod, *AIP Conf. Proc.* **1325**, 182, 2010
10. J. Xu, K.W. Plaxco, and S. J. Allen, Probing the collective vibrational dynamics of a protein in liquid water by terahertz absorption spectroscopy, *Protein Sci.* **15**, 1175, 2006
11. E. Castro-Camus, and M. B. Johnston, Conformational changes of photoactive yellow protein monitored by terahertz spectroscopy *Chem. Phys. Lett.*, **455**, 289, 2008
12. K. S. Yee, Numerical solution of initial boundary value problems involving Maxwell's equations in isotropic media, *IEEE Trans. Antenn. Propag.* **14**, 302, 1966.
13. 13. P. Bérenger, Perfectly Matched Layer (PML) for computational electromagnetics, Morgan & Claypool Publisher, 2007.
14. D. M. Sullivan, Electromagnetic simulation using the FDTD method, Wiley-IEEE Press, 2000
15. P. Markos, and C. M. Soukolis, Wave propagation from Electrons to Photonic Crystal and Left-Handed Material, Princeton University Press, 2008.
16. L. Peng, Absorption and emission properties of Photonic Crystals and Metamaterials, Thesis: Iowa State University, 2007.